Supplement: Aerosol Vertical Distributions Shaped by Boundary-Layer Dynamics in a Coastal-Urban Environment: Insights from TRACER

Bo Chen[1,2], Seth A. Thompson[1], Brianna H. Matthews[1,3], Milind Sharma[1], Ron Li[1], Anita D. Rapp[1], Christopher J. Nowotarski[1], and Sarah D. Brooks[1]

[1]Department of Atmospheric Sciences, Texas A&M University, College Station, 77843, United States
[2]now at Colorado State University, Fort Collins, Colorado, 80521, United States
[3]now at Savannah River National Laboratory, Aiken, South Carolina, 29808, United States

Correspondence to: Sarah D. Brooks (sbrooks@tamu.edu)

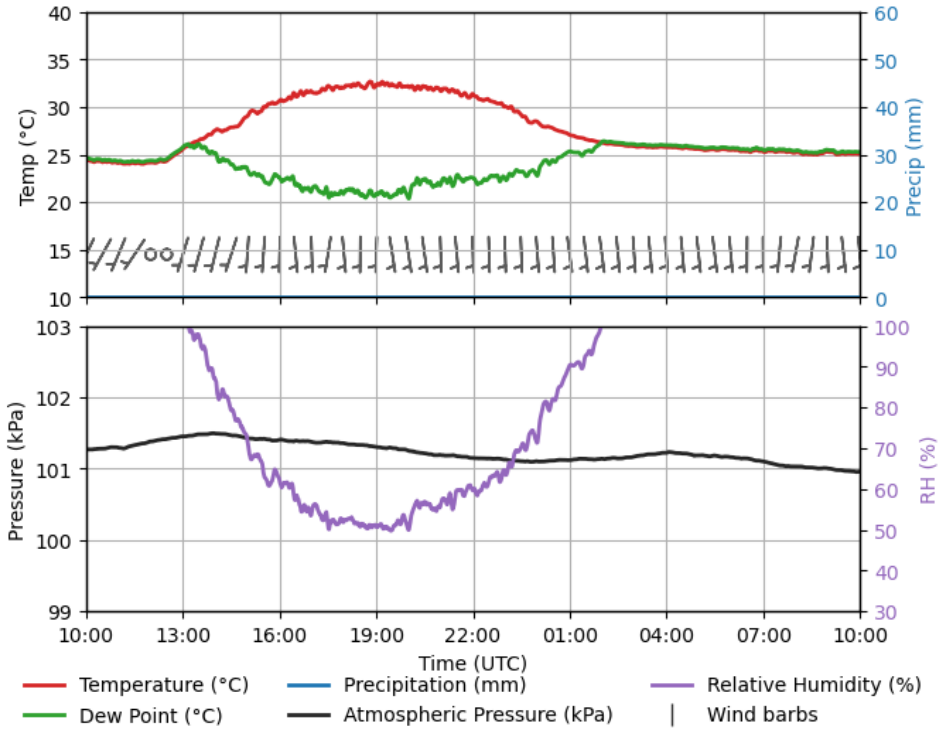

Figure S.1 Ground-based temperature, dewpoint, precipitation, wind (a), pressure, and relative humidity (b) measurements on 18 May 2022.

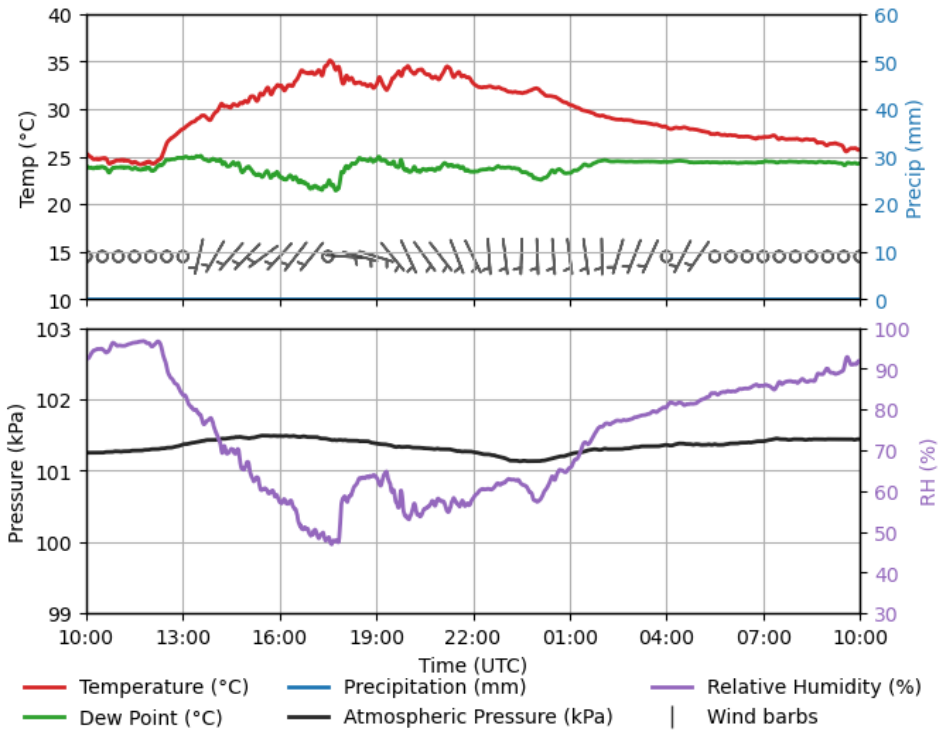

Figure S.2 Ground-based temperature, dewpoint, precipitation, wind (a), pressure, and relative humidity (b) measurements on 21 July 2022.

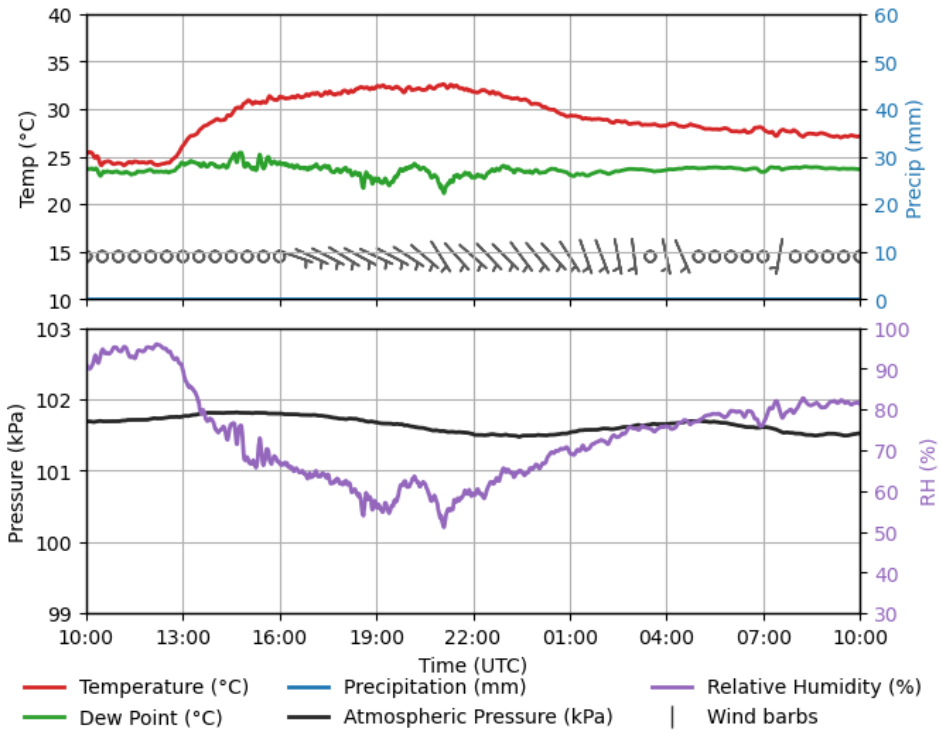

Figure S.3 Ground-based temperature, dewpoint, precipitation, wind (a), pressure, and relative humidity (b) measurements on 8 August 2022.

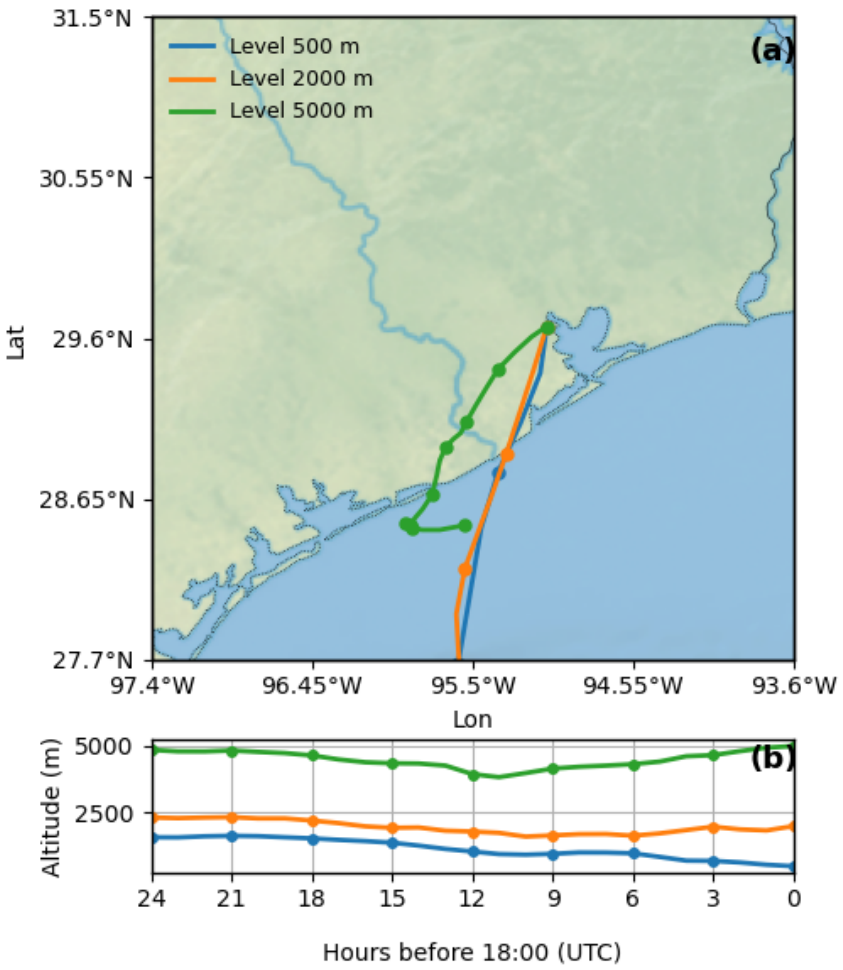

Figure S.4 HYSPLIT back trajectory evaluated for 18:00 on 18 May 2022, driven by HRRR meteorological fields (Stein et al., 2015).

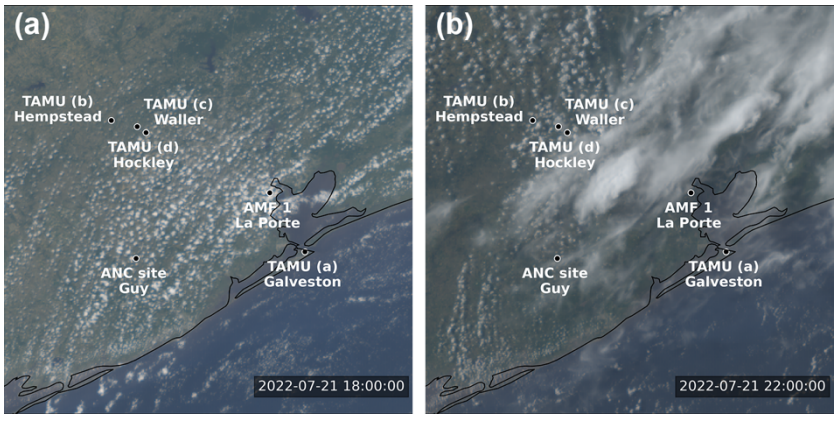

Figure S.5 GOES16 geocolor imagery on 21 July 2022, at UTC 18:00 (a) and 22:00 (b)

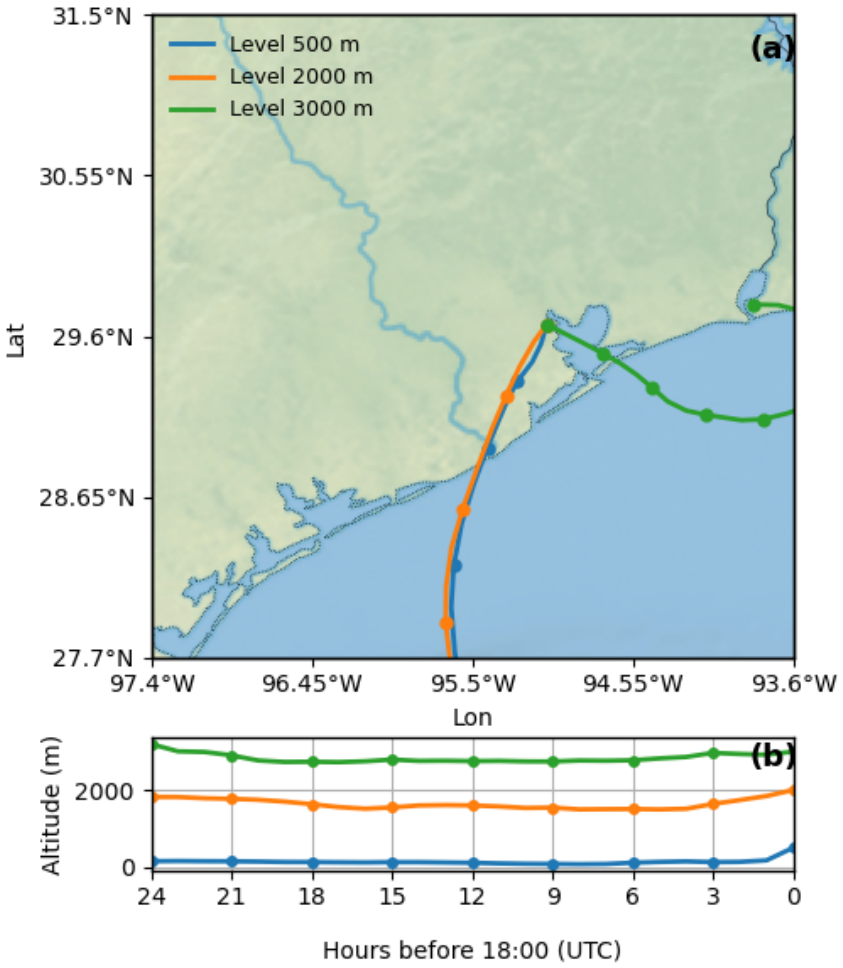

Figure S.6 HYSPLIT back trajectory evaluated for 18:00 on 21 July 2022, driven by HRRR meteorological fields (Stein et al., 2015).

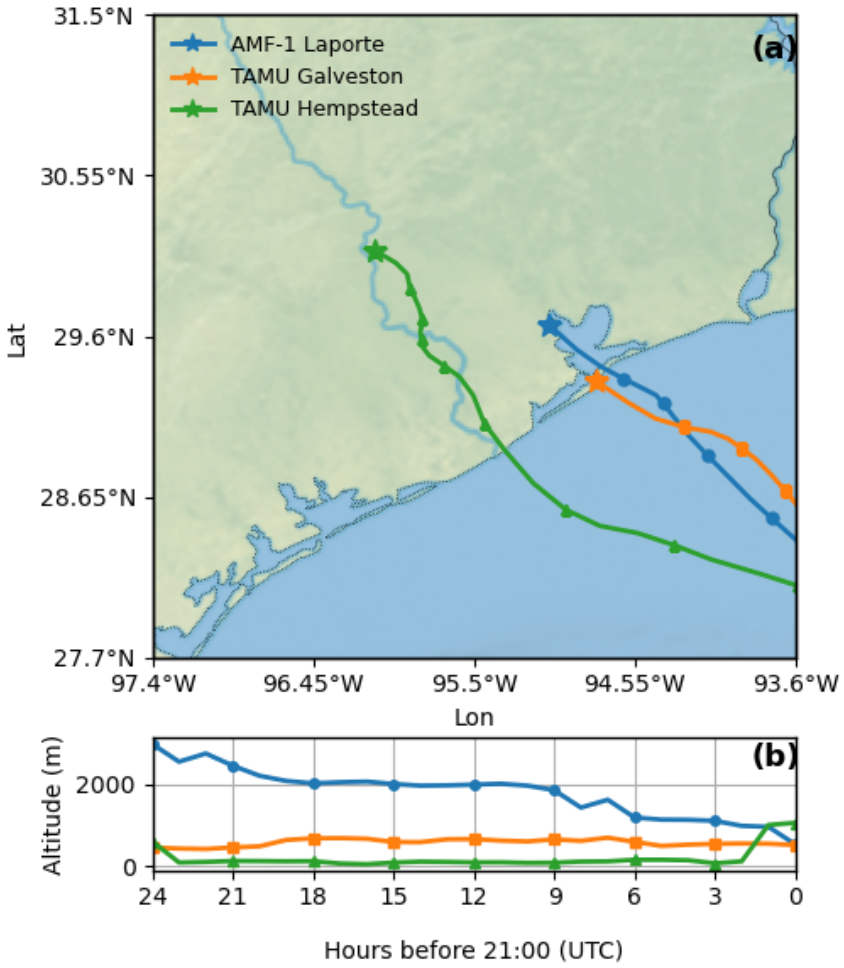

Figure S.7 HYSPLIT back trajectory evaluated for 21:00 on 8 August 2022, driven by HRRR meteorological fields (Stein et al., 2015).

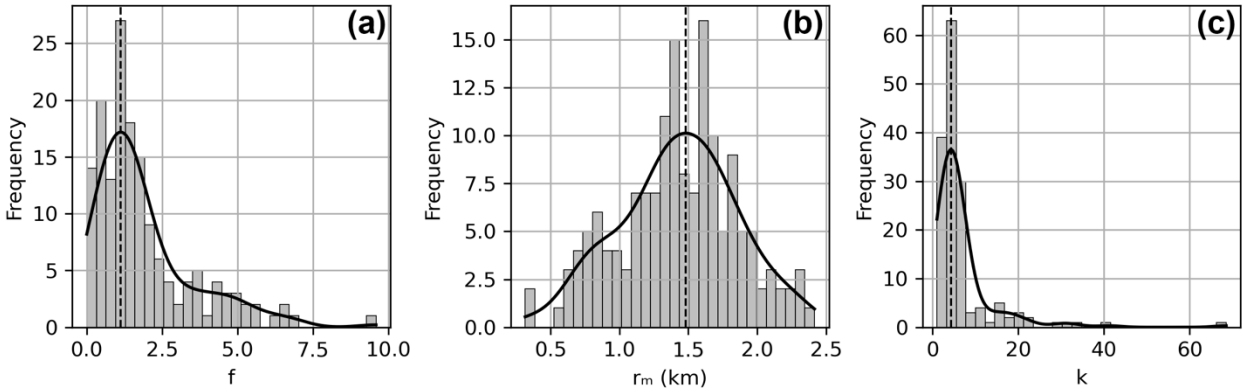

Figure S.8 Frequency distribution of fitted parameters. Gray bars show histograms of the fitted values, and the black line represents the kernel density estimate (KDE), a smoothed curve that approximates the underlying probability density of the data. The dashed vertical line marks the mode of the distribution (a) f (b) r_m (c) k

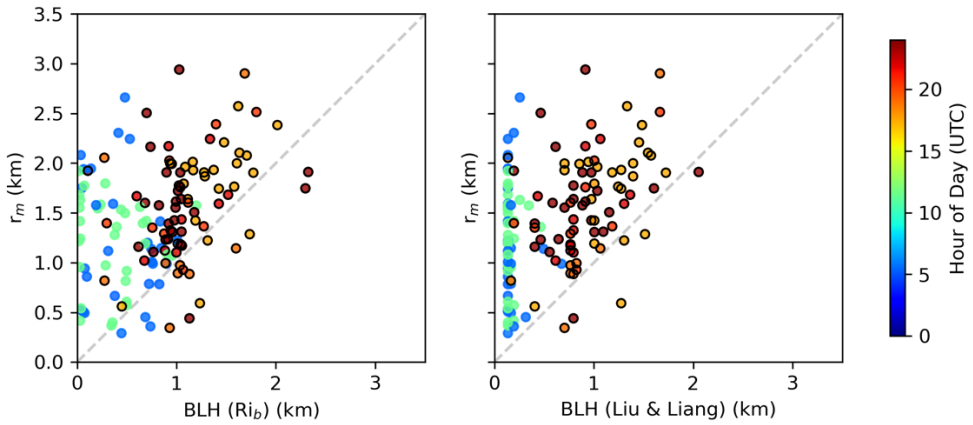

Figure S.9 Sensitivity of BLH–r_m comparison to fitting formulation (Equation 1 only). (a) Comparison between boundary-layer heights (BLH) derived from the bulk Richardson number method and the aerosol transition height r_m obtained from Equation 1 fits applied to all profiles. (b) Same as (a), but using BLH diagnosed with the Liu & Liang (2010) thermodynamic method. Scattered points are color coded by the hour of day (UTC), with warmer colors corresponding to daytime hours. Points corresponding to daytime hours (12:00–23:00 UTC) are additionally highlighted with black outlines.

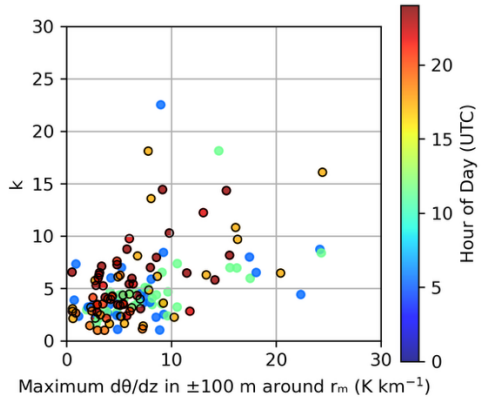

Figure S.10 Sensitivity of stability–k relationship to fitting formulation (Equation 1 only). Scatter plot comparing the local maximum potential temperature gradient, dθ/dz (evaluated within ±100 m of the aerosol transition height r_m), with the aerosol-profile sharpness parameter k derived from Equation 1 fits applied to all profiles for the ARM AMF-1 dataset. Points are color coded by the hour of day (UTC), with warmer colors corresponding to daytime hours. Points corresponding to daytime hours (12:00–23:00 UTC) are additionally highlighted with black outlines.

Table S.1

	10:59-11:59	17:00-18:00	23:00-00:00	05:00-06:00
BLH(R_{ib}) (km)	0.86	1.17	0.95	0.94
BLH(L&L) (km)	0.14	0.97	0.85	0.32
$d\theta/dz(R_{ib})$ (°C/km)	90.75	43.49	89.06	58.98
$d\theta/dz$(L&L) (°C/km)	11.24	66.49	68.98	11.65
X_0 (cm^{-3})	1901.50	1556	1680.87	1566.33
X_C (cm^{-3})	101.56	92.61	74.59	82.68
r_m (km)	0.92	1.1	1.07	0.99
k	44.10	13.24	33.17	60.66
γ	0.3	0.3	0.3	0.3
f	0.58	0.59	0.58	0
R^2	0.9736	0.9783	0.9773	0.9836

Table S.2

	11:00-12:00	17:00-18:00	22:59-23:59	04:59-05:59
BLH(R_{ib}) (km)	0.38	1.77	0.89	0.7
BLH(Liu&Liang) (km)	0.14	1.73	0.85	0.2
$d\theta/dz(R_{ib})$ (°C/km)	5.25	11.06	13.5	15.05
$d\theta/dz$(L&L) (°C/km)	24.97	11.06	10.83	11.16
X_0 (cm^{-3})	1723.37	2039.65	2519.54	1815.73
X_C (cm^{-3})	20.05	122.57	120	175.56
r_m (km)	1.12	1.94	2.04	1.09
k	6.37	7.09	11.55	4.79
γ	0.3	0.3	0.3	0.3
f	0.56	1.22	0.94	0
R^2	0.9954	0.9857	0.9714	0.9517

Table S.3

	10:58-11:58	17:00-18:00	18:30-19:30	21:30-22:30	05:04-06:04
BLH(R_{ib}) (km)	0.02	1.19	0.89	0.88	0.51
BLH(L&L) (km)	0.14	1	0.82	0.77	0.28
$d\theta/dz(R_{ib})$ (°C/km)	127.23	12.43	12.94	2.68	6.03
$d\theta/dz$(L&L) (°C/km)	39.53	19.99	12.94	58.94	5.50
X_0 (cm^{-3})	4371.69	7166.14	3907.51	2947.41	3770.95
X_C (cm^{-3})	51.17	357.57	93.24	143.05	55.1
r_m (km)	1.18	1.26	1.16	1.11	1.29
k	4.51	2.3	1.66	2.83	3.91
γ	0.3	0.3	0.3	0.3	0.3
f	1.13	0.38	0.51	0.44	1.24
R^2	0.9951	0.9954	0.9932	0.9861	0.9832

Table S.4

	16:14-18:47 (TAMU)	21:09-22:55 (TAMU)
BLH(R_{ib}) (km)	1.27	2.55
BLH(Liu&Liang) (km)	1.25	2.6
$d\theta/dz(R_{ib})$ (°C/km)	9.94	5.97
$d\theta/dz$(L&L) (°C/km)	9.94	5.1
X_0 (cm^{-3})	2246.68	6736.45
X_C (cm^{-3})	72.76	119.12
r_m (km)	0.94	1.94
k	3.03	2.56
γ	0.3	0.3
f	0.9	2.56
R^2	0.9959	0.9896

Reference

Stein, A. F., Draxler, R. R., Rolph, G. D., Stunder, B. J., Cohen, M. D., and Ngan, F.: NOAA's HYSPLIT atmospheric transport and dispersion modeling system, Bulletin of the American Meteorological Society, 96, 2059-2077, 2015.